

## CONTRAST ENHANCEMENT IN DERMOSCOPY IMAGES BY MAXIMIZING A HISTOGRAM BIMODALITY MEASURE

*M. Emre Celebi\**

Dept. of Computer Science  
Louisiana State University  
Shreveport, LA, USA  
ecelebi@lsu.edu

*Hitoshi Iyatomi*

Dept. of Electrical Informatics  
Hosei University  
Tokyo, Japan  
iyatomi@hosei.ac.jp

*Gerald Schaefer*

Dept. of Computer Science  
Loughborough University  
Loughborough, UK  
G.Schaefer@lboro.ac.uk

### ABSTRACT

Dermoscopy is one of the major imaging modalities used in the diagnosis of melanoma and other pigmented skin lesions. Due to the difficulty and subjectivity of human interpretation, automated analysis of dermoscopy images has become an important research area. Border detection is typically the first step in this analysis yet is often limited by the quality of the images to be analyzed. In this paper, we present an effective method to enhance the contrast in dermoscopy images. Given an input RGB image, we determine the optimal weights to convert it to grayscale by maximizing a histogram bimodality measure. Experiments on a large set of images demonstrate that this adaptive optimization scheme increases the contrast between the lesion and the background skin, and leads to a more accurate separation of the two regions using Otsu's thresholding method.

**Index Terms**—Melanoma, dermoscopy, border detection, contrast enhancement, Otsu's thresholding method

### 1. INTRODUCTION

Malignant melanoma, the most deadly form of skin cancer, is one of the most rapidly increasing cancers in the world, with an estimated incidence of 62,480 and an estimated total of 8,420 deaths in the United States in 2008 alone [1]. Early diagnosis is particularly important since melanoma can be cured with a simple excision if detected early.

Dermoscopy has become one of the most important tools in the diagnosis of melanoma and other pigmented skin lesions. This non-invasive skin imaging technique involves optical magnification, which makes subsurface structures more easily visible when compared to conventional clinical images [2]. This in turn reduces screening errors and provides greater differentiation between difficult lesions such as pigmented Spitz nevi and small, clinically equivocal lesions [3]. However, it has also been demonstrated that dermoscopy may ac-

tually lower the diagnostic accuracy in the hands of inexperienced dermatologists [4]. Therefore, in order to minimize the diagnostic errors that result from the difficulty and subjectivity of visual interpretation, the development of computerized image analysis techniques is of paramount importance [5, 6].

Automated border detection is often the first step in the automated analysis of dermoscopy images [7]. It is crucial for the image analysis for two main reasons. First, the border structure provides important information for accurate diagnosis, as many clinical features, such as asymmetry, border irregularity, and abrupt border cutoff, are calculated directly from the border. Second, the extraction of other important clinical features such as atypical pigment networks, globules, and blue-white areas, critically depends on the accuracy of border detection. Automated border detection is a challenging task due to several reasons: (i) low contrast between the lesion and the surrounding skin, (ii) irregular and fuzzy lesion borders, (iii) artifacts and intrinsic cutaneous features such as black frames, skin lines, blood vessels, hairs, and air bubbles, and (iv) variegated coloring inside the lesion.

Several preprocessing methods have been developed to facilitate the detection of lesion borders in dermoscopy images. Most of these methods focused on the removal of artifacts such as hairs [5, 8, 9, 10, 11] and bubbles [5]. Delgado *et al.* [12] proposed a contrast enhancement method based on independent histogram pursuit. Recently, Celebi *et al.* [13] proposed a method for approximate lesion localization using an ensemble of thresholding algorithms.

In this paper, we present an effective method to enhance the contrast in dermoscopy images. Given an input RGB image, we determine the optimal weights to convert it to grayscale by maximizing a histogram bimodality measure. We demonstrate that this image-dependent optimization scheme increases the contrast between the lesion and the background skin, and leads to a more accurate separation of the two regions using Otsu's thresholding method.

The rest of the paper is organized as follows. Section 2 describes Otsu's thresholding method, the histogram bimodality measure, and the proposed contrast enhancement method.

\*This publication was made possible by a grant from The Louisiana Board of Regents (LEQSF2008-11-RD-A-12).

Section 3 presents the experimental results. Finally, Section 4 gives the conclusions.

## 2. CONTRAST ENHANCEMENT BY MAXIMIZING HISTOGRAM BIMODALITY

Given an image represented in  $L$  gray levels  $\{0, 1, \dots, L-1\}$ , Otsu's thresholding method [14] partitions the image pixels into two classes  $C_1 = \{0, 1, \dots, t^*\}$  and  $C_2 = \{t^*+1, t^*+2, \dots, L-1\}$  (object and background, or vice versa) at gray level:

$$t^* = \operatorname{argmax}_{t \in \{0, 1, \dots, L-1\}} \sigma_B^2(t) \quad (1)$$

that maximizes the between-class variance  $\sigma_B^2(t)$  given by:

$$\begin{aligned} \sigma_B^2(t) &= p_1(t)p_2(t) [\mu_1(t) - \mu_2(t)]^2 \\ p(i) &= \frac{n_i}{n}, p_1(t) = \sum_{i=0}^t p(i), p_2(t) = 1 - p_1(t) \\ \mu(t) &= \sum_{i=0}^t ip(i), \mu_1(t) = \frac{\mu(t)}{p_1(t)}, \mu_2(t) = \frac{\mu_T - \mu(t)}{p_2(t)} \end{aligned} \quad (2)$$

where  $n_i$  is the number of pixels with gray level  $i$ ,  $n = \sum_{i=0}^{L-1} n_i$  is the total number of pixels,  $p_1$  and  $p_2$  are the class probabilities,  $\mu_1$  and  $\mu_2$  are the class means, and  $\mu_T = \mu(L-1)$  is the total mean gray level.

Between-class variance (BCV) can be viewed as a measure of class separability or histogram bimodality. It can be explicitly calculated as:

$$\sigma_B^2(t) = \frac{[\mu_T p_1(t) - \mu(t)]^2}{p_1(t)p_2(t)} \quad (3)$$

which can be made invariant to affine transformations of the gray level scale by dividing it by the total variance  $\sigma_T^2$ :

$$\sigma_T^2 = \sum_{i=0}^{L-1} (i - \mu_T)^2 p(i) \quad (4)$$

In this study, normalized BCV, i.e.  $\sigma_B^2(t)/\sigma_T^2$ , is used as a measure of histogram bimodality. Note that normalized BCV values fall into the  $[0, 1]$  range.

As mentioned in §1, one of the factors that complicate the detection of borders in dermoscopy images is insufficient contrast. We propose Algorithm 1 to increase the contrast between the lesion and the background skin. This algorithm takes two inputs: an RGB image  $X$  with  $n$  three-component pixels  $\mathbf{x} = [r, g, b]$  (r: red, g: green, b:blue) and a set  $W$  of  $m$  three-component weight vectors  $\mathbf{w} = [w_r, w_g, w_b]$ . It outputs an image  $Y^*$ , which is a grayscale contrast-enhanced version of  $X$ .  $Y^*$  is obtained by converting  $X$  to grayscale using the optimal weight vector  $\mathbf{w}^* \in W$ , which is the vector that gives the highest normalized BCV value. In other words,

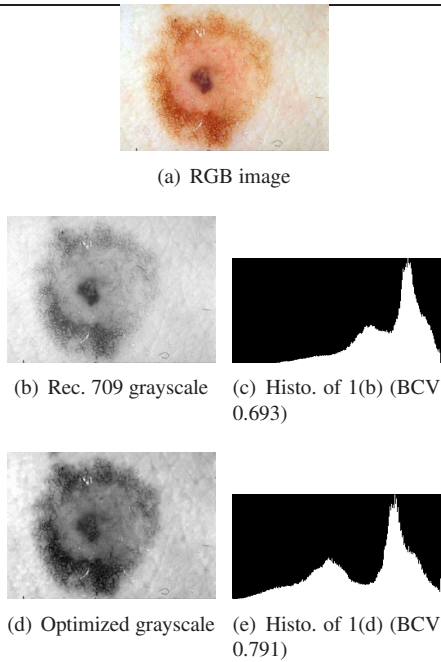
$Y^*$  is the grayscale version of  $X$ , in which the object and its background are maximally separated.

## 3. EXPERIMENTAL RESULTS AND DISCUSSION

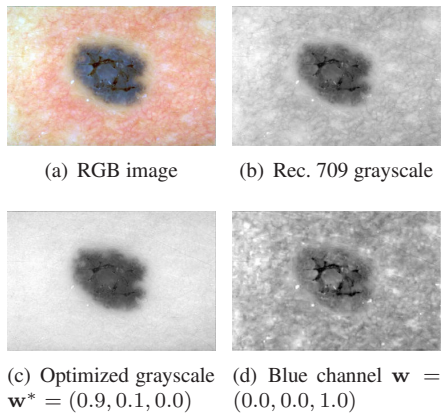
The only parameter involved in Algorithm 1 is the set of weight vectors  $W$ , which essentially constitutes the search space of the procedure. It is tempting to think that better class separability could be obtained with a larger search space at the expense of increased computational time. However, small perturbations in the optimal weight vector do not necessarily modify the shape of histogram enough to give substantially different normalized BCV values. In our experiments, we observed that choosing the component weights from  $\{0.1, 0.2, \dots, 1.0\}$  often ensures that the highest possible normalized BCV values are attained. Note that a feasible weight vector  $\mathbf{w} = [w_r, w_g, w_b]$  must satisfy the constraint  $w_r + w_g + w_b = 1.0$  in order to produce valid luminance values, e.g. values in the  $[0, 255]$  range for 8-bit images.

Figure 1 shows the effect of the contrast enhancement operation on the histogram of a dermoscopy image. Parts 1(b) and 1(c) show the ITU Recommendation 709 (Rec. 709) ( $\mathbf{w} = [0.2126, 0.7152, 0.0722]$ ) grayscale version of the input image and its histogram, respectively. Parts 1(d) and 1(e) show the optimized ( $\mathbf{w}^* = [0.0, 0.0, 1.0]$ ) grayscale version of the input image and its histogram, respectively. It can be seen that the presented contrast enhancement procedure effectively increases the class separability, which results in higher contrast between the lesion and the background skin. This improvement in the contrast is also reflected by a 14% increase in the normalized BCV and a 25% increase in the distance between the histogram modes. Interestingly, the optimized weight vector puts no emphasis on the red and green channels. However, experiments on a set of 367 dermoscopy images revealed that such a blue-dominant weighting scheme is not necessarily optimal (see Figure 2).

Figure 3 shows the influence of the contrast enhancement operation on thresholding results. In each row, the first column represents the original RGB image, the second and third columns contain the Otsu thresholding outputs for the grayscale images obtained using the Rec. 709 and the optimized weight vector, respectively. It can be seen that, in each case, the presented contrast enhancement method leads to a better thresholding result. It should be noted that in many cases it is still necessary to perform post-processing to determine the lesion border [7]. Table 1 shows the normalized BCV, optimal threshold ( $t^*$ ), and border detection error (XOR) values for the images in Figure 3. The XOR value is given by  $\frac{\text{Area}(AB \oplus MB)}{\text{Area}(MB)} 100\%$ , where  $AB$  is the Otsu thresholding output,  $MB$  is the border drawn by an expert dermatologist,  $\oplus$  is the exclusive-OR operation that gives the pixels for which  $AB$  and  $MB$  disagree, and  $\text{Area}(I)$  denotes the number of pixels in the binary image  $I$ .



**Fig. 1.** Influence of contrast enhancement on histogram bimodality



**Fig. 2.** A case where red-dominant weighting gives the best separation

In order to test the influence of contrast enhancement on border detection, we applied the proposed method to a set of 367 dermoscopy images. The average XOR error for the Rec. 709 grayscale images thresholded by Otsu’s method was 20.147%, whereas the error for the optimized grayscale images was 16.561%, which represents a significant improvement. It should be noted that no post-processing was performed in each case.

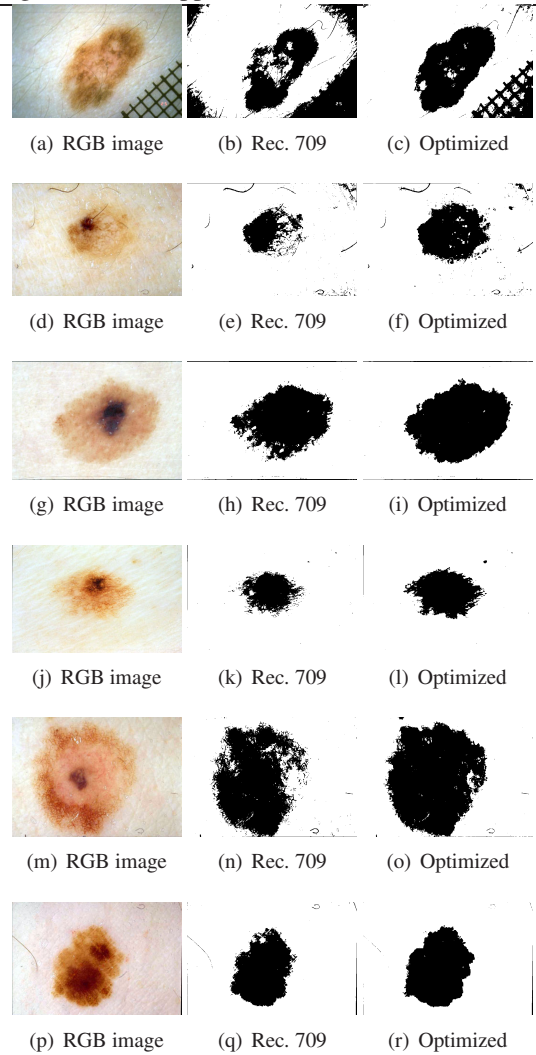


**Fig. 3.** Influence of contrast enhancement on thresholding

#### 4. CONCLUSIONS

In this paper, an effective method for contrast enhancement in dermoscopy images is presented. The method iteratively searches for the optimal RGB to grayscale conversion weights that maximize Otsu’s histogram bimodality measure. Experiments on a large set of dermoscopy images demonstrated that the presented optimization scheme, in general, leads to better thresholding results and lower border detection errors. The execution time of the method is about 0.2 seconds for a typical image of size  $768 \times 512$  pixels on an Intel®Core™2 Quad Q6700 2.66 GHz machine.

#### 5. REFERENCES

[1] A. Jemal, R. Siegel, and E. Ward *et al.*, “Cancer Statistics, 2008,” *Cancer J Clin*, vol. 58, pp. 71–96, 2008.

**Table 1.** Statistics for Figure 3

Image	Rec. 709 grayscale			Optimized grayscale		
	BCV	$t^*$	XOR (%)	BCV	$t^*$	XOR (%)
3(a)	0.610	166	39.249	0.739	137	20.088
3(d)	0.528	178	11.039	0.638	153	3.892
3(g)	0.724	191	24.264	0.860	175	14.422
3(j)	0.705	191	12.204	0.799	162	6.681
3(m)	0.706	182	29.830	0.791	153	15.914
3(p)	0.811	152	9.059	0.901	126	4.711

```

input :  $X = \{\mathbf{x}_1, \mathbf{x}_2, \dots, \mathbf{x}_n\}$ 
          $W = \{\mathbf{w}_1, \mathbf{w}_2, \dots, \mathbf{w}_m\}$ 
output:  $Y^* = \{y_1^*, y_2^*, \dots, y_n^*\}$ 
 $bcv^* = 0$ 
foreach  $\mathbf{w} = [w_r, w_g, w_b] \in W$  do
  Convert  $X$  to  $Y$  using  $\mathbf{w}$ ;
  foreach  $\mathbf{x}_i = [r_i, g_i, b_i] \in X$  do
     $y_i = w_r \cdot r_i + w_g \cdot g_i + w_b \cdot b_i$ 
  end
  Reset the histogram  $h$  of  $Y$ ;
  for ( $g = 0$ ;  $g < L$ ;  $g = g + 1$ ) do
     $h[g] = 0$ 
  end
  Populate  $h$ ;
  foreach  $y_i \in Y$  do
     $h[y_i] = h[y_i] + 1$ 
  end
  Calculate the normalized BCV;
   $bcv = \text{calc\_bcv}(h)$ 
  if  $bcv^* < bcv$  then
     $\mathbf{w}$  gives the best normalized BCV so far;
     $bcv^* = bcv$ 
     $\mathbf{w}^* = \mathbf{w}$ 
  end
end
Convert  $X$  to  $Y^*$  using  $\mathbf{w}^* = [w_r^*, w_g^*, w_b^*]$ ;
foreach  $\mathbf{x}_i = [r_i, g_i, b_i] \in X$  do
   $y_i^* = w_r^* \cdot r_i + w_g^* \cdot g_i + w_b^* \cdot b_i$ 
end

```

**Algorithm 1:** Contrast enhancement by maximizing Otsu’s histogram bimodality measure

- [2] G. Argenziano, H.P. Soyer, and V. De Giorgi, *Dermoscopy: A Tutorial*, EDRA Medical Publishing & New Media, 2002.
- [3] K. Steiner, M. Binder, and M. Schemper *et al.*, “Statistical Evaluation of Epiluminescence Dermoscopy Criteria for Melanocytic Pigmented Lesions,” *J Am Acad Dermatol*, vol. 29, pp. 581–588, 1993.
- [4] M. Binder, M. Schwarz, and A. Winkler *et al.*, “Epiluminescence Microscopy. A Useful Tool for the Diagnosis of Pigmented Skin Lesions for Formally Trained Dermatologists,” *Arch Dermatol*, vol. 131, pp. 286–291, 1995.
- [5] M.G. Fleming, C. Steger, and J. Zhang *et al.*, “Techniques for a Structural Analysis of Dermoscopic Imagery,” *Comput Med Imaging Graphics*, vol. 22, pp. 375–389, 1998.
- [6] M.E. Celebi, H.A. Kingravi, and B. Uddin *et al.*, “A Methodological Approach to the Classification of Dermoscopy Images,” *Comput Med Imaging Graphics*, vol. 31, pp. 362–373, 2007.
- [7] M.E. Celebi, H. Iyatomi, G. Schaefer, and W.V. Stoecker, “Lesion Border Detection in Dermoscopy Images,” *Comput Med Imaging Graphics*, vol. 33, pp. 148–153, 2009.
- [8] T.K. Lee, V. Ng, and R. Gallagher *et al.*, “Dullrazor: A Software Approach to Hair Removal from Images,” *Comput Bio Med*, vol. 27, pp. 533–543, 1997.
- [9] P. Schmid, “Segmentation of Digitized Dermoscopic Images by Two-Dimensional Color Clustering,” *IEEE Trans Med Imaging*, vol. 18, pp. 164–171, 1999.
- [10] H. Zhou, M. Chen, and R. Gass, “Feature-Preserving Artifact Removal from Dermoscopy Images,” in *Proc of the SPIE Med Imaging Conf*, 2008, vol. 6914 of *SPIE*.
- [11] P. Wighton, T.K. Lee, and M.S. Atkins, “Dermoscopic Hair Disocclusion Using Inpainting,” in *Proc. of the SPIE Medical Imaging Conf*, 2008, vol. 6914 of *SPIE*.
- [12] D. Delgado, C. Butakoff, B.K. Ersboll, and W.V. Stoecker, “Independent Histogram Pursuit for Segmentation of Skin Lesions,” *IEEE Trans Biomed Eng*, vol. 55, pp. 157–161, 2008.
- [13] M.E. Celebi, H. Iyatomi, G. Schaefer, and W.V. Stoecker, “Approximate Lesion Localization in Dermoscopy Images,” *Skin Res Technol*, vol. 15, pp. 314–322, 2009.
- [14] N. Otsu, “A Threshold Selection Method from Gray Level Histograms,” *IEEE Trans SMC*, vol. 9, pp. 62–66, 1979.